

A COMPARATIVE STUDY FOR THE NUCLEAR NORMS MINIMIZATION METHODS

Zhiyuan Zha^{1,2}, Bihan Wen², Jiachao Zhang³, Jiantao Zhou⁴ and Ce Zhu¹

¹School of Information and Communication Engineering,
University of Electronic Science and Technology of China, Chengdu, 611731, China.

²School of Electrical and Electronic Engineering, Nanyang Technological University, 639798, Singapore.

³Kangni Mechanical and Electrical Institute, Nanjing Institute of Technology, Nanjing 211167, China.

⁴Department of Computer and Information Science, University of Macau, Macau 999078, China.

ABSTRACT

The nuclear norm minimization (NNM) is commonly used to approximate the matrix rank by shrinking all singular values equally. However, the singular values have clear physical meanings in many practical problems, and NNM may not be able to faithfully approximate the matrix rank. To alleviate the above-mentioned limitation of NNM, recent studies have suggested that the weighted nuclear norm minimization (WNNM) can achieve a better rank estimation than NNM, which heuristically set the weight being inverse to the singular values. However, it still lacks a rigorous explanation why WNNM is more effective than NNM in various applications. In this paper, we analyze NNM and WNNM from the perspective of group sparse representation (GSR). Concretely, an adaptive dictionary learning method is devised to connect the rank minimization and GSR models. Based on the proposed dictionary, we prove that NNM and WNNM are equivalent to ℓ_1 -norm minimization and the weighted ℓ_1 -norm minimization in GSR, respectively. Inspired by enhancing sparsity of the weighted ℓ_1 -norm minimization in comparison with ℓ_1 -norm minimization in sparse representation, we thus explain that WNNM is more effective than NNM. By integrating the image nonlocal self-similarity (NSS) prior with the WNNM model, we then apply it to solve the image denoising problem. Experimental results demonstrate that WNNM is more effective than NNM and outperforms several state-of-the-art methods in both objective and perceptual quality.

Index Terms— Low-rank matrix approximation, NNM, WNNM, GSR, image denoising.

1. INTRODUCTION

Due to the fact that the data from many practical cases has low-rank property, such as video [1] and hyperspectral image [2], low-rank matrix approximation (LRMA) has shown great potentials in various applications including image processing [3, 4], computer vision [5–7] and machine learning [8–12]. For instance, the foreground and background in a video are modeled as low-rank and sparse [5, 6], respectively.

The Netflix customer data matrix is treated as low-rank, since the customers' behaviors and attributes are highly correlated, thus can be modeled by a few principle components.

Generally speaking, there are two popular approaches for LRMA: low-rank matrix factorization (LRMF) [8, 9] and rank minimization [3, 4, 7, 10–12]. In this paper, we focus on the rank minimization methods, with the nuclear norm minimization (NNM) [10, 12] being the representative one. The goal of NNM is to recover the underlying low-rank matrix X from its degraded observation Y , by minimizing the nuclear norm of X . In recent years, various applications based on NNM have been developed, such as image/video denoising [1, 4], background extraction [5, 6] and face shadow removal [13, 14]. However, the nuclear norm is usually adopted as a convex surrogate of the matrix rank. Though possessing the theoretical guarantee, NNM tries to shrink different rank components equally, and therefore it cannot estimate the matrix rank accurately enough. To mitigate the disadvantage of NNM, a variety of enhanced low-rank approximation methods have been proposed [3, 7, 11, 14–16]. In particular, the most well-known one is the weighted nuclear norm minimization (WNNM) model [3, 7], which assigns different weights to different singular values such that the matrix rank approximation becomes more accurate than NNM. However, it still lacks a rigorous explanation why WNNM is more effective than NNM in various applications.

Based on the above concern in mind, this paper explains why WNNM is more effective than NNM model from the point of group sparse representation (GSR). To the best of our knowledge, this is the first work to propose a rigorous explanation why WNNM is more effective than NNM. Specifically, we firstly devise an adaptive dictionary learning method to connect the rank minimization and GSR models. Then, we prove that under the proposed dictionary, NNM and WNNM are equivalent to ℓ_1 -norm minimization and the weighted ℓ_1 -norm minimization in GSR, respectively. Encouraged by enhancing sparsity of the weighted ℓ_1 -norm minimization in comparison with ℓ_1 -norm minimization in sparse representation, we then indicate that WNNM is more effective than

NNM. We employ the WNNM model to image denoising along with image nonlocal self-similarity (NSS) [17] prior. Experimental results demonstrate that WNNM is more effective than NNM and outperforms many state-of-the-art denoising methods.

2. RELATED WORKS

2.1. Nuclear Norm Minimization

According to [10, 12], the nuclear norm is the tightest convex relaxation of the original rank minimization problem. Given a data matrix $\mathbf{Y}_i \in \mathbb{R}^{b \times c}$, NNM aims to find a matrix $\mathbf{X}_i \in \mathbb{R}^{b \times c}$ of rank r , which can be formulated as the following minimization problem,

$$\mathcal{D}_\lambda(\mathbf{Y}_i) = \arg \min_{\mathbf{X}_i} \frac{1}{2} \|\mathbf{Y}_i - \mathbf{X}_i\|_F^2 + \lambda \|\mathbf{X}_i\|_*, \quad (1)$$

where $\|\mathbf{X}_i\|_* = \sum_j \sigma_{i,j}$, and $\sigma_{i,j}$ is the j -th singular value of the matrix \mathbf{X}_i . λ is a positive constant.

2.2. Weighted Nuclear Norm Minimization

Although a good theoretical guarantee by the singular value thresholding (SVT) model [10], NNM tends to over-shrink the rank components, and therefore, it achieves unsatisfactory accuracy for approximating the matrix rank. To improve the rank approximation performance of NNM, Gu *et al.* [3, 7] proposed the WNNM model. To be concrete, the weighted nuclear norm $\|\mathbf{X}_i\|_{\mathbf{W}_i,*}$ is used to regularize \mathbf{X}_i . Then, Eq. (1) can be rewritten as

$$\mathcal{D}_{\mathbf{W}_i}(\mathbf{Y}_i) = \arg \min_{\mathbf{X}_i} \frac{1}{2} \|\mathbf{Y}_i - \mathbf{X}_i\|_F^2 + \|\mathbf{X}_i\|_{\mathbf{W}_i,*} \quad (2)$$

where $\|\mathbf{X}_i\|_{\mathbf{W}_i,*} = \sum_j w_{i,j} \sigma_{i,j}$, $\mathbf{W}_i = \text{diag}(w_{i,1}, w_{i,2}, \dots, w_{i,j})$, $m = \min(b, c)$, $\forall j = 1, \dots, m$, and $w_{i,j} > 0$ is a non-negative weight assigned to $\sigma_{i,j}$.

3. ANALYZING NNM AND WNNM BASED ON THE GROUP SPARSE REPRESENTATION

In this section, we analyze NNM and WNNM from the point of GSR. We first introduce the GSR model.

3.1. Group Sparse Representation

Instead of using a single patch as the basic unit in patch sparse representation (PSR) [18, 19], the GSR model considers each similar *patch group* as the basic unit and has shown great potentials in various image processing tasks [20–24]. The GSR provides a powerful mechanism to integrate local sparsity and NSS of images. To be concrete, an image \mathbf{x} with size $\sqrt{N} \times \sqrt{N}$ is divided into n overlapped patches \mathbf{x}_i of size $\sqrt{b} \times \sqrt{b}$, $i = 1, 2, \dots, n$. Then, we use each patch \mathbf{x}_i as a reference patch, and impose an $L \times L$ sized searching window that is centered at \mathbf{x}_i . K-Nearest Neighbour (KNN) algorithm [25] is used to select c most similar patches (based on their Euclidean distance to the reference patch) to form a

set \mathcal{S}_i . Following this, all the patches in \mathcal{S}_i are stacked into a data matrix $\mathbf{X}_i \in \mathbb{R}^{b \times c}$, which contains each element of \mathcal{S}_i as its column, *i.e.*, $\mathbf{X}_i = \{\mathbf{x}_{i,1}, \mathbf{x}_{i,2}, \dots, \mathbf{x}_{i,c}\}$. This matrix \mathbf{X}_i consisting of patches with similar structures is thereby called a *patch group*, where $\{\mathbf{x}_{i,j}\}_{j=1}^c$ denotes the j -th patch in the i -th *patch group*. Similar to PSR [18, 19], given a dictionary \mathbf{D}_i , each *patch group* \mathbf{X}_i can be sparsely represented by solving the following ℓ_0 -norm minimization problem,

$$\hat{\mathbf{A}}_i = \arg \min_{\mathbf{A}_i} \left(\frac{1}{2} \|\mathbf{X}_i - \mathbf{D}_i \mathbf{A}_i\|_F^2 + \lambda \|\mathbf{A}_i\|_0 \right), \quad (3)$$

where \mathbf{A}_i represents the group sparse coefficient of each *patch group* \mathbf{X}_i . $\|\cdot\|_F^2$ denotes the Frobenius norm, and $\|\cdot\|_0$ signifies the ℓ_0 -norm, *i.e.*, counting the nonzero entries of each column in \mathbf{A}_i .

However, since ℓ_0 -norm minimization problem is a difficult combinatorial optimization problem, solving Eq. (3) is NP-hard. Therefore, Eq. (3) is usually relaxed to the convex ℓ_1 -norm minimization counterpart, *i.e.*,

$$\hat{\mathbf{A}}_i = \arg \min_{\mathbf{A}_i} \left(\frac{1}{2} \|\mathbf{X}_i - \mathbf{D}_i \mathbf{A}_i\|_F^2 + \lambda \|\mathbf{A}_i\|_1 \right), \quad (4)$$

However, in some practical problems, such as image inverse problems [1, 22], ℓ_1 -norm minimization is quite hard to achieve a sparse solution accurately, and thus leads to a poor reconstruction performance. This raises the question of whether we can improve the sparsity of ℓ_1 -norm minimization or not. In other words, we wish that ℓ_1 -norm minimization can be an alternative to ℓ_0 -norm minimization and achieve a better solution. For this reason, Candès *et al.* [26] proposed a well-known norm minimization method, *i.e.*, the weighted ℓ_1 -norm minimization, and instead of Eq. (4), we have the following minimization problem,

$$\hat{\mathbf{A}}_i = \arg \min_{\mathbf{A}_i} \left(\frac{1}{2} \|\mathbf{X}_i - \mathbf{D}_i \mathbf{A}_i\|_F^2 + \|\mathbf{W}_i \circ \mathbf{A}_i\|_1 \right), \quad (5)$$

where \circ represents the element-wise product of two matrices, here \mathbf{W}_i is a weight assigned to each \mathbf{A}_i and it can enhance the representation capability of \mathbf{A}_i . Note that the weight \mathbf{W}_i is inversely proportional to \mathbf{A}_i [26]. Meanwhile, we have the following conjecture.

Conjecture 1. [26] *Defining the weighted ℓ_1 -norm minimization $\mathbf{v}_1 = \arg \min_{\mathbf{x} \in \mathbb{R}^n} \|\mathbf{W}\mathbf{x}\|_1$ and ℓ_1 -norm minimization $\mathbf{v}_2 = \arg \min_{\mathbf{x} \in \mathbb{R}^n} \|\mathbf{x}\|_1$, then we have,*

$$\mathbf{v}_1 \succ \mathbf{v}_2, \quad (6)$$

where the weight \mathbf{W} is inversely proportional to $|\mathbf{x}|$. $\mathbf{v}_1 \succ \mathbf{v}_2$ denotes that the entry \mathbf{v}_1 has much more sparsity encouraging than the entry \mathbf{v}_2 .

In order to explain why WNNM is more effective than NNM model, we analyze them from the point of GSR. We first introduce an adaptive dictionary learning method.

3.2. Adaptive Dictionary Learning

In this subsection, we present an adaptive dictionary learning method. For each *patch group* X_i , its adaptive dictionary can be learned from its observation $Y_i \in \mathbb{R}^{b \times c}$. Specifically, we apply the singular value decomposition (SVD) to Y_i ,

$$Y_i = U_i \Delta_i V_i^T = \sum_{j=1}^m \delta_{i,j} \mathbf{u}_{i,j} \mathbf{v}_{i,j}^T, \quad (7)$$

where $\Delta_i = \text{diag}(\delta_{i,1}, \delta_{i,2}, \dots, \delta_{i,m})$ is a diagonal matrix, $m = \min(b, c)$, $\forall j = 1, \dots, m$, and $\mathbf{u}_{i,j}, \mathbf{v}_{i,j}$ are the columns of U_i and V_i , respectively.

Following this, we define each dictionary atom $\mathbf{d}_{i,j}$ of the adaptive dictionary D_i for each *patch group* Y_i , namely, $\mathbf{d}_{i,j} = \mathbf{u}_{i,j} \mathbf{v}_{i,j}^T$, $\forall j = 1, \dots, m$. We then have learned an adaptive dictionary, *i.e.*,

$$D_i = [\mathbf{d}_{i,1}, \mathbf{d}_{i,2}, \dots, \mathbf{d}_{i,m}] \quad (8)$$

It can be seen that the proposed dictionary learning method only needs one SVD operation per *patch group*.

3.3. WNNM is More Effective than NNM

Now, recalling the adaptive dictionary defined in Eq. (8), given the degraded matrix Y_i , ℓ_1 -norm minimization based on GSR model can be represented as

$$\hat{A}_i = \arg \min_{A_i} \left(\frac{1}{2} \|Y_i - D_i A_i\|_F^2 + \lambda \|A_i\|_1 \right), \quad (9)$$

Similarly, given the degraded matrix Y_i , then the weighted ℓ_1 -norm minimization based on GSR model can be formulated as the following minimization problem,

$$\hat{A}_i = \arg \min_{A_i} \left(\frac{1}{2} \|Y_i - D_i A_i\|_F^2 + \|W_i \circ A_i\|_1 \right), \quad (10)$$

According to the above design of the adaptive dictionary D_i in Eq. (8), we have the following conclusions.

Theorem 1. *The NNM in Eq. (1) is equivalent to the ℓ_1 -norm minimization in Eq. (9) under the proposed adaptive dictionary D_i .*

Corollary 1. *The WNNM in Eq. (2) is equivalent to the weighted ℓ_1 -norm minimization in Eq. (10) under the proposed adaptive dictionary D_i .*

Then, based on Theorem 1, Corollary 1, and assuming the correctness of Conjecture 1, we have the following proposition.

Proposition 1. *Defining the weighted nuclear norm minimization $\mathbf{h}_1 = \arg \min_{X_i} \|X_i\|_{w_i, *}$ and the nuclear norm minimization $\mathbf{h}_2 = \arg \min_{X_i} \|X_i\|_*$, then we have*

$$\mathbf{h}_1 \gg \mathbf{h}_2. \quad (11)$$

where $\mathbf{h}_1 \gg \mathbf{h}_2$ denotes that the entry \mathbf{h}_1 is more effective than the corresponding entry \mathbf{h}_2 . It is noted that the weight is inversely proportional to the singular value of X_i .

Based on Proposition 1, we have thus explained why WNNM is more effective than NNM model. Note that, there are a variety of methods to devise the dictionary and the proposed adaptive dictionary learning approach is just one of them. Though the proposed dictionary learning seems to directly translate the sparse representation into the rank minimization problem, the main difference between the sparse representation and rank minimization models (*e.g.*, NNM [10] and WNNM [3]) is that sparse representation has a dictionary learning operator, while the rank minimization problem does not, to the best of our knowledge.

4. GSR-WNNM FOR IMAGE DENOISING

Since the GSR model is exploited to analyze the effectiveness of WNNM, we termed the proposed scheme as GSR-WNNM. In this section, to validate the effectiveness of WNNM model, we employ the GSR-WNNM model to solve the image denoising problem. Mathematically, image denoising [27–31] aims to restore the clean image \mathbf{x} from its noisy observation \mathbf{y} , which can be generally modeled as $\mathbf{y} = \mathbf{x} + \mathbf{n}$, where \mathbf{n} is usually assumed to be additive white Gaussian noise. In this work, we use the image NSS prior [17] with the GSR-WNNM model to image denoising. The NSS prior indicates that many similar patches can be searched for any exemplar patch by natural images within nonlocal regions. Specifically, each patch \mathbf{y}_i is extracted from the degraded image \mathbf{y} . Like in the subsection 3.1, we search for its c nonlocal similar patches to generate a *patch group* Y_i , *i.e.*, $Y_i = \{\mathbf{y}_{i,1}, \mathbf{y}_{i,2}, \dots, \mathbf{y}_{i,c}\}$. Then we have $Y_i = X_i + N_i$, where X_i and N_i are the group matrices of original image and noise, respectively. Since all the patches in each data matrix have similar structures, the constructed data matrix Y_i has a low-rank property and we can use the low-rank approximation method to estimate X_i from Y_i . Then, by invoking the GSR-WNNM model, each *patch group* X_i can be reconstructed by solving the following optimization problem,

$$\hat{X}_i = \arg \min_{X_i} \left(\frac{1}{2} \|Y_i - X_i\|_F^2 + \|X_i\|_{w_i, *} \right). \quad (12)$$

Then, the closed-form solution of Eq. (12) can be solved by

$$\sigma_{i,j} = \text{soft}(\delta_{i,j}, w_{i,j}) = \max(\delta_{i,j} - w_{i,j}, 0), \quad (13)$$

where $Y_i = U_i \Delta_i V_i^T$ is the SVD of $Y_i \in \mathbb{R}^{b \times c}$ with $\Delta_i = \text{diag}(\delta_{i,1}, \dots, \delta_{i,m})$, $m = \min(b, c)$, $\forall j = 1, \dots, m$. $X_i = U_i \Sigma_i V_i^T$ is the SVD of X_i with $\Sigma_i = \text{diag}(\sigma_{i,1}, \dots, \sigma_{i,m})$.

With the solution of Σ_i in Eq. (13), the clean group matrix \hat{X}_i can be recovered as $\hat{X}_i = U_i \Sigma_i V_i^T$. Then the clean image $\hat{\mathbf{x}}$ can be reconstructed by aggregating all the groups $\{\hat{X}_i\}$.

The weight W_i of each *patch group* X_i is usually set to be inverted to the singular values, and thus, in [3], the weight is heuristically set as $w_{i,j} = q/(\sigma_{i,j} + \varepsilon)$, where q and ε are the constant. However, WNNM model in [3]

sometimes ejects the terminating error. In this paper, we present an adaptive weight setting scheme to avoid this error. Specifically, inspired by [32], the weight \mathbf{W}_i of each *patch group* $\hat{\mathbf{X}}_i$ is set as $\mathbf{w}_i = [w_{i,1}, w_{i,2}, \dots, w_{i,j}]$. We have $\mathbf{w}_i = q * 2\sqrt{2}\sigma_n^2 / (\gamma_i + \varepsilon)$, where σ_n^2 represents the noise variance, and γ_i denotes the estimated standard variance of the singular values of each *patch group*. The complete description of the GSR-WNNM for image denoising is exhibited in Algorithm 1.

Algorithm 1 The GSR-WNNM for image denoising.

Require: Noisy image \mathbf{y} .

- 1: Initialize $\hat{\mathbf{x}}^0 = \mathbf{y}, \mathbf{y}^0 = \mathbf{y}$.
 - 2: **for** $k = 0$ **to** K **do**
 - 3: Iterative regularization $\mathbf{y}^k = \hat{\mathbf{x}}^{k-1} + \mu(\mathbf{y} - \hat{\mathbf{x}}^{k-1})$;
 - 4: **for** Each patch \mathbf{y}_i in \mathbf{y}^k **do**
 - 5: Find nonlocal similar patches to form a *patch group* \mathbf{Y}_i ;
 - 6: Singular value decomposition $[\mathbf{U}_i, \mathbf{\Delta}_i, \mathbf{V}_i] = \text{SVD}(\mathbf{Y}_i)$;
 - 7: Estimate the weight \mathbf{w}_i of each *patch group* by compute $\mathbf{w}_i = q * 2\sqrt{2}\sigma_n^2 / (\gamma_i + \varepsilon)$;
 - 8: Calculate $\mathbf{\Sigma}_i$ by Eq. (13);
 - 9: Reconstruct $\hat{\mathbf{X}}_i = \mathbf{U}_i \mathbf{\Sigma}_i \mathbf{V}_i^T$;
 - 10: **end for**
 - 11: Aggregate $\hat{\mathbf{X}}_i$ to form the restored image $\hat{\mathbf{x}}^k$.
 - 12: **end for**
 - 13: **Output:** The final denoised image $\hat{\mathbf{x}}$.
-



Fig. 1. All test images.

5. EXPERIMENTAL RESULTS

In this section, we conduct experiments to validate the performance of the GSR-WNNM for image denoising. To verify the effectiveness of WNNM model, we compare it with NNM model (dubbed GSR-NNM in our work). All experimental test images are shown in Fig. 1. The source code is available at: <https://drive.google.com/open?id=1ZAkBCMPxIzgZ36y4zs-kg9ot7kqXnuHD>.

We compare the GSR-WNNM with some leading denoising methods, including BM3D [20], EPLL [27], Plow [29], NCSR [28], PGPD [23], OGLR [30] and GSR-NNM methods. The averaged PSNR values of the GSR-WNNM, as well as the selected competing methods are shown in Table 1. The averaged PSNR gains of the GSR-WNNM over BM3D, EPLL, NCSR, Plow, PGPD, OGLR and GSR-NNM methods are 0.32dB, 0.82dB, 0.44dB, 0.85dB, 0.21dB, 0.55dB and 1.50dB, respectively. It is clear that the GSR-WNNM significantly outperforms the GSR-NNM method. Therefore, this result is consistent with our above theoretical analysis. A denoising example in the case of $\sigma_n = 100$ for image *Leaves* is shown in Fig. 2. It can be seen that over-smooth effects or undesirable artifacts are generated by BM3D, EPLL, NCSR, Plow, PGPD, OGLR and GSR-NNM methods. The

GSR-WNNM improves the quality of the denoised images by significantly reducing artifacts and over-smooth effects. Therefore, these results demonstrate that WNNM is more effective than NNM model and also validate the superior of the WNNM model.

Table 1. Average PSNR results (dB) of different methods.

Noise Level	20	30	40	50	75	100
BM3D [20]	31.64	29.65	28.04	27.09	25.17	23.81
EPLL [27]	31.19	29.14	27.69	26.58	24.58	23.21
Plow [29]	31.03	29.19	27.79	26.67	24.53	23.01
NCSR [28]	31.65	29.54	28.10	26.99	24.92	23.45
PGPD [23]	31.71	29.69	28.29	27.22	25.26	23.87
OGLR [30]	31.47	29.54	28.14	26.85	24.87	23.14
GSR-NNM	30.29	28.37	27.52	26.14	23.92	22.04
GSR-WNNM	31.89	29.91	28.51	27.41	25.45	24.13

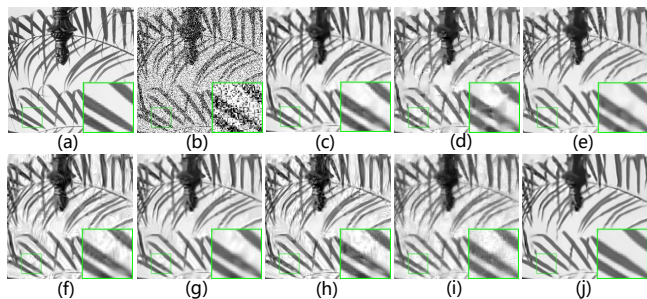


Fig. 2. Denoising performance comparison of image *Leaves* with $\sigma_n = 100$. (a) Original image; (b) Noisy image; (c) BM3D (PSNR = 20.90dB); (d) EPLL (PSNR = 20.26dB); (e) NCSR (PSNR = 20.84dB); (f) Plow (PSNR = 20.43dB); (g) PGPD (PSNR = 20.95dB); (h) OGLR (PSNR = 20.28dB); (i) GSR-NNM (PSNR = 19.57dB); (j) GSR-WNNM (PSNR = **21.56dB**).

6. CONCLUSION

This paper proposed a comparative study for the nuclear norms minimization methods. We have devised an adaptive dictionary learning method to connect the rank minimization and GSR models. Based on the proposed adaptive dictionary, we have proved that NNM and WNNM are equivalent to ℓ_1 -norm minimization and the weighted ℓ_1 -norm minimization in GSR, respectively. Following this, inspired by the correctness of enhancing sparsity of the weighted ℓ_1 -norm in comparison with ℓ_1 -norm in sparse representation, we have explained that WNNM is more effective than NNM. We have applied the GSR-WNNM model with image NSS prior to image denoising. Experimental results have demonstrated that WNNM is more effective than NNM and outperforms many state-of-the-art methods both quantitatively and qualitatively.

7. ACKNOWLEDGE

This work was supported by the NSFC (61571102), the applied research programs of science and technology., Sichuan Province (No. 2018JY0035), the Ministry of Education, Republic of Singapore, under the Start-up Grant and the Macau Science and Technology Development Fund under Grant FDCT/077/2018/A2.

References

- [1] H. Ji, C. Liu, Z. Shen, and Y. Xu, "Robust video denoising using low rank matrix completion," in *2010 IEEE Computer Society Conference on Computer Vision and Pattern Recognition*, June 2010, pp. 1791–1798.
- [2] H. Zhang, W. He, L. Zhang, H. Shen, and Q. Yuan, "Hyperspectral image restoration using low-rank matrix recovery," *IEEE Transactions on Geoscience and Remote Sensing*, vol. 52, no. 8, pp. 4729–4743, 2014.
- [3] S. Gu, L. Zhang, W. Zuo, and X. Feng, "Weighted nuclear norm minimization with application to image denoising," in *Proceedings of the IEEE Conference on Computer Vision and Pattern Recognition*, 2014, pp. 2862–2869.
- [4] W. Dong, G. Shi, and X. Li, "Nonlocal image restoration with bilateral variance estimation: a low-rank approach," *IEEE transactions on image processing*, vol. 22, no. 2, pp. 700–711, 2013.
- [5] J. Wright, A. Ganesh, S. Rao, Y. Peng, and Y. Ma, "Robust principal component analysis: Exact recovery of corrupted low-rank matrices via convex optimization," in *Advances in neural information processing systems*, 2009, pp. 2080–2088.
- [6] Y. Peng, A. Ganesh, J. Wright, W. Xu, and Y. Ma, "Rasl: Robust alignment by sparse and low-rank decomposition for linearly correlated images," *IEEE transactions on pattern analysis and machine intelligence*, vol. 34, no. 11, pp. 2233–2246, 2012.
- [7] S. Gu, Q. Xie, D. Meng, W. Zuo, X. Feng, and L. Zhang, "Weighted nuclear norm minimization and its applications to low level vision," *International Journal of Computer Vision*, vol. 121, no. 2, pp. 183–208, 2017.
- [8] G. Liu, Z. Lin, S. Yan, J. Sun, Y. Yu, and Y. Ma, "Robust recovery of subspace structures by low-rank representation," *IEEE transactions on pattern analysis and machine intelligence*, vol. 35, no. 1, pp. 171–184, 2013.
- [9] Y. Zheng, G. Liu, S. Sugimoto, S. Yan, and M. Okutomi, "Practical low-rank matrix approximation under robust l_1 -norm," in *Computer Vision and Pattern Recognition (CVPR), 2012 IEEE Conference on*. IEEE, 2012, pp. 1410–1417.
- [10] J. Cai, E. J. Candès, and Z. Shen, "A singular value thresholding algorithm for matrix completion," *SIAM Journal on Optimization*, vol. 20, no. 4, pp. 1956–1982, 2010.
- [11] C. Lu, C. Zhu, C. Xu, S. Yan, and Z. Lin, "Generalized singular value thresholding," in *AAAI*, 2015, pp. 1805–1811.
- [12] M. Fazel, *Matrix rank minimization with applications*, Ph.D. thesis, PhD thesis, Stanford University, 2002.
- [13] Y. Mu, J. Dong, X. Yuan, and S. Yan, "Accelerated low-rank visual recovery by random projection," in *Computer Vision and Pattern Recognition (CVPR), 2011 IEEE Conference on*. IEEE, 2011, pp. 2609–2616.
- [14] Z. Kang, C. Peng, and Q. Cheng, "Robust pca via nonconvex rank approximation," in *Proceedings of the 2015 IEEE International Conference on Data Mining (ICDM)*. IEEE Computer Society, 2015, pp. 211–220.
- [15] Y. Hu, D. Zhang, J. Ye, X. Li, and X. He, "Fast and accurate matrix completion via truncated nuclear norm regularization," *IEEE transactions on pattern analysis and machine intelligence*, vol. 35, no. 9, pp. 2117–2130, 2013.
- [16] T. H. Oh, Y. Tai, J. C. Bazin, H. Kim, and I. S. Kweon, "Partial sum minimization of singular values in robust pca: Algorithm and applications," *IEEE transactions on pattern analysis and machine intelligence*, vol. 38, no. 4, pp. 744–758, 2016.
- [17] A. Buades, B. Coll, and J. M. Morel, "A non-local algorithm for image denoising," in *Computer Vision and Pattern Recognition, 2005. CVPR 2005. IEEE Computer Society Conference on*. IEEE, 2005, vol. 2, pp. 60–65.
- [18] M. Elad and M. Aharon, "Image denoising via sparse and redundant representations over learned dictionaries," *IEEE Transactions on Image processing*, vol. 15, no. 12, pp. 3736–3745, 2006.
- [19] M. Aharon, M. Elad, and A. Bruckstein, "K-svd: An algorithm for designing overcomplete dictionaries for sparse representation," *IEEE Transactions on signal processing*, vol. 54, no. 11, pp. 4311, 2006.
- [20] K. Dabov, A. Foi, V. Katkovnik, and K. Egiazarian, "Image denoising by sparse 3-d transform-domain collaborative filtering," *IEEE Transactions on image processing*, vol. 16, no. 8, pp. 2080–2095, 2007.
- [21] J. Mairal, F. Bach, J. Ponce, G. Sapiro, and A. Zisserman, "Non-local sparse models for image restoration," in *Computer Vision, 2009 IEEE 12th International Conference on*. IEEE, 2009, pp. 2272–2279.
- [22] J. Zhang, D. Zhao, and W. Gao, "Group-based sparse representation for image restoration," *IEEE Transactions on Image Processing*, vol. 23, no. 8, pp. 3336–3351, 2014.
- [23] J. Xu, L. Zhang, W. Zuo, D. Zhang, and X. Feng, "Patch group based nonlocal self-similarity prior learning for image denoising," in *Proceedings of the IEEE international conference on computer vision*, 2015, pp. 244–252.
- [24] Q. Wang, X. Zhang, Y. Wu, L. Tang, and Z. Zha, "Nonconvex weighted ℓ_p minimization based group sparse representation framework for image denoising," *IEEE Signal Processing Letters*, vol. 24, no. 11, pp. 1686–1690, 2017.
- [25] J. M. Keller, M. R. Gray, and J. A. Givens, "A fuzzy k-nearest neighbor algorithm," *IEEE transactions on systems, man, and cybernetics*, , no. 4, pp. 580–585, 1985.
- [26] E. J. Candes, M. B. Wakin, and S. P. Boyd, "Enhancing sparsity by reweighted ℓ_1 minimization," *Journal of Fourier analysis and applications*, vol. 14, no. 5-6, pp. 877–905, 2008.
- [27] D. Zoran and Y. Weiss, "From learning models of natural image patches to whole image restoration," in *Computer Vision (ICCV), 2011 IEEE International Conference on*. IEEE, 2011, pp. 479–486.
- [28] W. Dong, L. Zhang, G. Shi, and X. Li, "Nonlocally centralized sparse representation for image restoration," *IEEE Transactions on Image Processing*, vol. 22, no. 4, pp. 1620–1630, 2013.
- [29] P. Chatterjee and P. Milanfar, "Patch-based near-optimal image denoising," *IEEE Transactions on Image Processing*, vol. 21, no. 4, pp. 1635, 2012.
- [30] J. Pang and G. Cheung, "Graph laplacian regularization for image denoising: Analysis in the continuous domain," *IEEE Transactions on Image Processing*, vol. 26, no. 4, pp. 1770–1785, 2017.
- [31] B. Wen, S. Ravishanker, and Y. Bresler, "Structured overcomplete sparsifying transform learning with convergence guarantees and applications," *International Journal of Computer Vision*, vol. 114, no. 2-3, pp. 137–167, 2015.
- [32] S. G. Chang, B. Yu, and M. Vetterli, "Adaptive wavelet thresholding for image denoising and compression," *IEEE transactions on image processing*, vol. 9, no. 9, pp. 1532–1546, 2000.